Summer 2011

Upgrade and simulation of the subcritical assembly at Missouri University of Science and Technology

Lucas Powelson Tucker

Follow this and additional works at: https://scholarsmine.mst.edu/masters_theses

Part of the Nuclear Engineering Commons

Department:

Recommended Citation

Tucker, Lucas Powelson, "Upgrade and simulation of the subcritical assembly at Missouri University of Science and Technology" (2011). *Masters Theses*. 4979.

https://scholarsmine.mst.edu/masters_theses/4979

UPGRADE AND SIMULATION OF THE

SUBCRITICAL ASSEMBLY AT

MISSOURI UNIVERSITY OF SCIENCE AND TECHNOLOGY

by

LUCAS POWELSON TUCKER

A THESIS

Presented to the Faculty of the Graduate School of the

MISSOURI UNIVERSITY OF SCIENCE AND TECHNOLOGY

In Partial Fulfillment of the Requirements of the Degree

MASTER OF SCIENCE IN NUCLEAR ENGINEERING

2011

Approved by

Shoaib Usman, Advisor
Arvind Kumar
Carlos H. Castaño
Hyoung Lee

PUBLICATION THESIS OPTION

This thesis consists of the journal article that will be submitted for publication to Nuclear Engineering & Design Journal. Pages 1-22 of this thesis have been prepared in the style utilized by the Nuclear Engineering & Design Journal.

ABSTRACT

The Missouri University of Science and Technology Subcritical Assembly (S&TSub) was brought back into service and upgraded with a new neutron detection system and internet access. Before the upgrade neutron counting was only possible in one location. Using a movable detection system housed in acrylic tubes measurements can now be taken in any empty fuel location and at any height within the tube, making three dimensional flux mapping a possibility. By connecting the new detection system to a Canberra Lynx Digital Signal Analyzer, remote users can have limited data collecting capabilities. To further enhance the potential of the facility, an MCNP model of the S&TSub was created, and validated by comparing its simulated predictions to experiments conducted at the facility. An approach to criticality experiment using the 1/M approximation showed that the MCNP model accurately predicts k_{eff} if the detectors are place between 27 cm and 36 cm from the neutron source. The results of an axial flux measurement experiment differed from the MCNP simulated results by an average of 12%. Finally, the validated MCNP model was used to show the effect of removing the facility's fixed detector tube and redistributing its fuel. MCNP simulation predicts that the new configuration would increase the multiplication factor from $0.73481 \pm 8.080E{-}05$ to $0.76844 \pm 4.610E{-}05$ and increase the flux magnitude by 36%.

ACKNOWLEDGEMENTS

TABLE OF CONTENTS

SECTION

APPENDICES

LIST OF ILLUSTRATIONS

LIST OF TABLES

Upgrade and Simulation of the Subcritical Assembly at Missouri University of Science and Technology

Lucas P. Tucker, Shoaib Usman[1], Ayodeji Alajo

Nuclear Engineering, Missouri University of Science and Technology, 203 Fulton Hall, 300W. 13th St., Rolla, MO-65409, United States

Abstract

The Missouri University of Science and Technology Subcritical Assembly (S&TSub) was brought back into service and upgraded with a new neutron detection system and internet access. Before the upgrade neutron counting was only possible in one location. Using a movable detection system housed in acrylic tubes measurements can now be taken in any empty fuel location and at any height within the tube, making three dimensional flux mapping a possibility. By connecting the new detection system to a Canberra Lynx Digital Signal Analyzer, remote users can have limited data collecting capabilities. To further enhance the potential of the facility, an MCNP model of the S&TSub was created, and validated by comparing its simulated predictions to experiments conducted at the facility. An approach to criticality experiment using the 1/M approximation showed that the MCNP model accurately predicts k_{eff} if the detectors are place between 27 cm and 36 cm from the neutron source. The results of an axial flux measurement experiment differed from the MCNP simulated results by an average of 12%. Finally, the validated MCNP model was used to show the effect of removing the facility's fixed detector tube and redistributing its fuel. MCNP simulation predicts that the new configuration would increase the multiplication factor from $0.73481\pm8.080\text{E-05}$ to $0.76844\pm4.610\text{E-05}$ and increase the flux magnitude by 36%.

Key Words: Subcritical Assembly, Internet accessible, [3]He neutron detector, MCNP

---

[1] Corresponding Author. Tel.: +1 573 341 4745; fax: +1 573 341 6309.
E-mail address: usmans@mst.edu (S. Usman).

1. Introduction

A subcritical assembly (SCA) is a nuclear pile that is generally fueled with natural uranium and moderated with light water making it incapable of maintaining a self-sustaining fission chain reaction without a supplementary neutron source. Though an SCA cannot be used for power generation, it is a useful teaching tool for nuclear engineering students. It can be used to demonstrate a reactor's neutron flux distribution and the impact of positive and negative reactivity insertion. The Missouri University of Science and Technology Subcritical Assembly (S&TSub) was purchased for the Nuclear Engineering Department in 1958 along with the requisite fuel and neutron source. The facility was installed in Fulton Hall for ease of access and remained there until 2007 when it was relocated to the Missouri S&T Reactor (MSTR) building. The facility has seen sporadic use lately. The purpose of the work described here was to return the S&TSub to full operational status, upgrade the facility with an internet accessible neutron detection system, model it with Monte Carlo N-Particle transport code (MCNP), validate the model experimentally, and use the validated model to assess potential adjustments to the facility.

2. S&TSub Characteristics

S&TSub was produced by the Nuclear Chicago Corporation. Figure 1A shows an axial cross section through the center of the facility with the major components labeled, while Table 1 lists some of its important dimensions. The core is housed in a 470 gallon tank made of stainless steel 316. The tank divides into two pieces across the mid-plane to make transportation easier, and a lead gasket is bolted between the two halves for water proofing. A stainless steel tube positioned on the lower half of the tank protrudes radially into the tank across the center, allowing detector access to the assembly. Two stainless steel grid plates allow fuel rods to be loaded in a regular hexagonal array. Each fuel rod is composed of five annular fuel slugs loaded into an aluminum guide tube. Each slug contains 1.8 kg of natural uranium metal and is clad in aluminum as seen in Figure 1B. The core can be loaded with up to 279 fuel rods.

2.1 Pu-Be Neutron Source Characteristics

During operation, a plutonium-beryllium neutron source is inserted into the pile. It is placed in a special guide tube at the center-most grid position that is not obstructed by the fixed detector tube. The neutron source is clad in tantalum and stainless steel and is mounted on the end of an acrylic rod to reduce exposure during its insertion and removal. Figure 1C shows the arrangement of the source, its cladding, its acrylic handle, and the source guide tube.
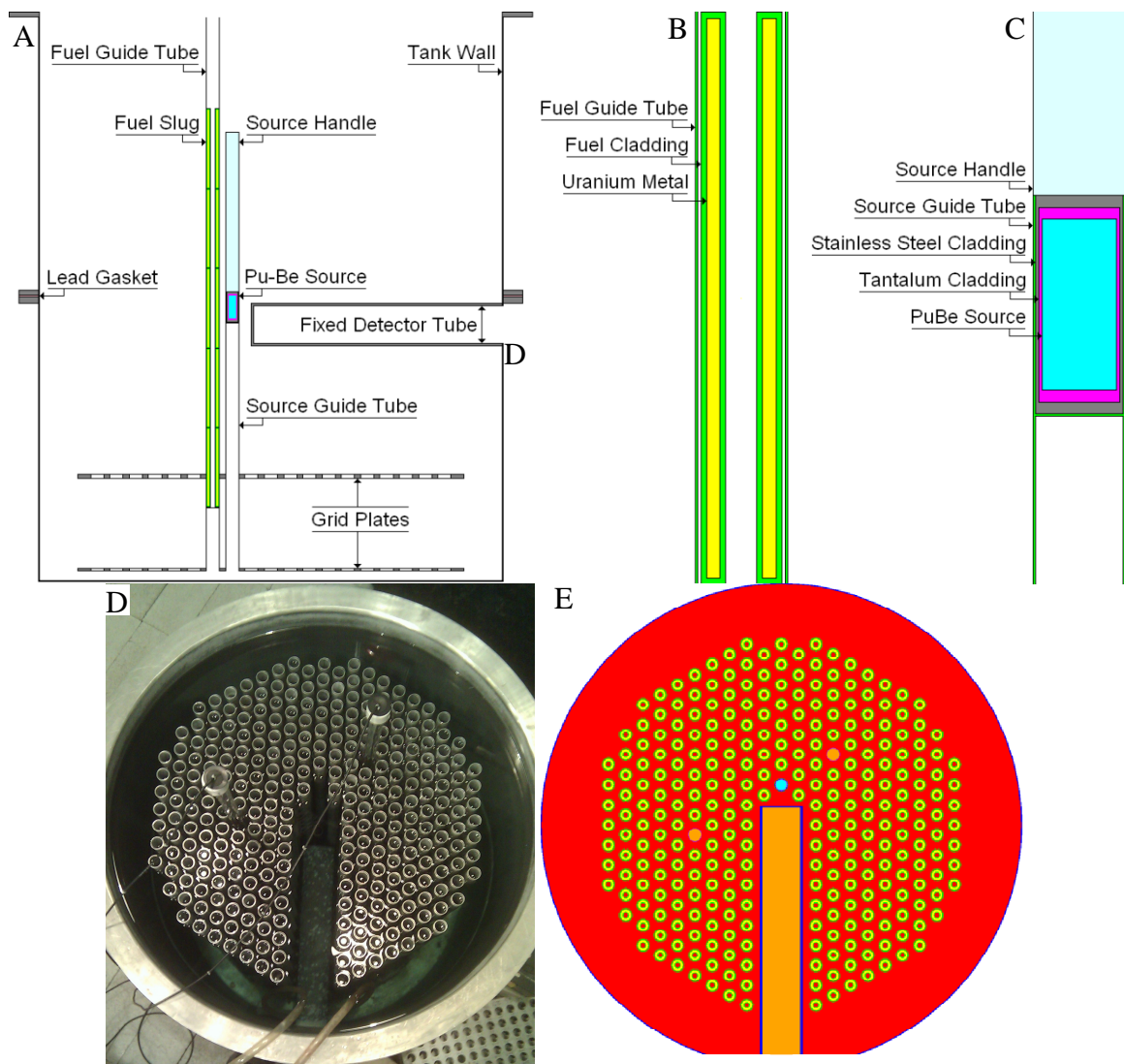
Fig. 1. S&TSub geometry. A. Axial cross section of S&TSub through its center. B. Axial cross section of a fuel slug and its guide tube. C. Axial cross section of the Pu-Be neutron source. D. Image of fully loaded S&TSub from above. E. Radial cross section

Table 1. Selected dimensions from S&TSub

Tank inner diameter	121.9 cm	Guide tube height	150.8 cm
Tank wall thickness	0.3 cm	Fuel height above tank bottom	19.8 cm
Tank height	152.4 cm	Fuel clad outer diameter	3.0 cm
Fixed detector tube centerline height	68.6 cm	Fuel clad inner diameter	1.2 cm
Fixed detector tube inner diameter	10.2 cm	Fuel clad length	21.4 cm
Fixed detector tube wall thickness	0.6 cm	Fuel clad thickness	0.2 cm
Bottom grid plate height	2.5 cm	Neutron source height	69.3 cm
Top grid plate height	27.3 cm	Neutron source diameter	2.8 cm
Pitch of hexagonal fuel array	2.5 cm	Neutron source length	6.4 cm
Guide tube diameter	3.5 cm	Tantalum source clad thickness	0.1 cm
Guide tube thickness	0.1 cm	Stainless steel source clad thickness	0.1 cm

2.2 Pu-Be Neutron Source Activity

In a Pu-Be source neutrons are produced by the ^{9}Be(α,n)^{12}C reaction, so the number of neutrons produced depends on the strength of the alpha source (Runnals and Boucher, 1956). There are five important isotopes of plutonium present in spent nuclear fuel – and subsequently a Pu-Be source – but each isotope's relative abundance depends on the initial enrichment of the fuel and its final burnup (Gunnink et al., 1974). Gunnink et al. reported the isotopic abundance of plutonium for several burnup values (1974). The primary decay mode for all of these nuclides – except ^{241}Pu – is alpha decay (Baum et al, 2002). ^{241}Pu decays by β^{-} emission to ^{241}Am, which is primarily an alpha emitter with a half-life of 432.7 years (Baum et al, 2002). As ^{241}Pu decays to ^{241}Am the alpha emission rate increases and the neutron emission rate increases concurrently. Tate and Coffinberry developed equation 1 to predict the increased neutron count rate (1958).

$$A(t) = A_0\left[1 + \Gamma\left(1 - e^{-t/\tau}\right)\right] \tag{1}$$

Where t is the time in years from the start of ^{241}Am accumulation

$A(t)$ is the neutron emission rate at time t

A_0 is the source activity before any ^{241}Am has accumulated

τ is the mean lifetime of ^{241}Pu

$$\Gamma = \frac{1.27\left[\dfrac{a\left(^{241}_{94}Pu\right)}{T\left(^{241}_{95}Am\right)}\right]}{\dfrac{a\left(^{239}_{94}Pu\right)}{T\left(^{239}_{94}Pu\right)}+\dfrac{a\left(^{240}_{94}Pu\right)}{T\left(^{240}_{94}Pu\right)}+1.27\left[\dfrac{a\left(^{238}_{94}Pu\right)}{T\left(^{238}_{94}Pu\right)}\right]}$$

Where *a* is the relative abundance and *T* is the half-life in years. The factor 1.27 corrects for the increased probability of neutron emission from the higher energy alpha particles emitted by [241]Am and [238]Pu.

Missouri S&T's neutron source was purchased at the same time as S&TSub in 1958. At that time, the source was composed of 37.68 g of beryllium and 76.27 g of plutonium, and it emitted $5.94*10^6$ n s^{-1}. However, the initial plutonium isotopic abundances are unknown. Table 2 reports several predicted source activities based Tate and Coffinberry's equation and the isotopic abundances measured at various values of fuel burnup by Gunnink et al.

Table 2. Pu-Be Neutron Source Activity from Fuel Burnup

Nuclide	$T_{1/2}$[a] (years)	Alpha Energy[a] (MeV)	Isotopic abundance (%) according to burnup[b]			
			8-10 GWd/t	16-18 GWd/t	25-27 GWd/t	38-40 GWd/t
[238]Pu	8.77E+01	5.4992	0.10	0.25	1.0	2.0
[239]Pu	2.41E+04	5.156	87	75	58	45
[240]Pu	6.56E+03	5.1683	10	18	25	27
[241]Pu	1.44E+01	β decay	2.4	4.5	9.0	15.0
[242]Pu	3.75E+05	4.901	0.3	1.0	7.0	12.0
Activity (n s^{-1})			1.45E+07	4.10E+07	1.66E+08	4.43E+08

[a](Baum et al., 2002)   [b](Gunnink et al., 1974)

2.3 Pu-Be Neutron Source Energy Spectrum

Measuring the neutron energy spectrum of the source was beyond the scope of this project, so a spectrum adapted from the work of Kumar and Nagarajan was used (1977). The spectrum is plotted in figure 2. Kumar and Nagarajan used cross-section values, material properties, and alpha decay energies and rates to calculate the neutron emission spectrum from a Pu-Be source with an assumed [239]Pu enrichment of 100%. The change in the neutron energy spectrum due to the decay of [241]Pu discussed above was ignored.
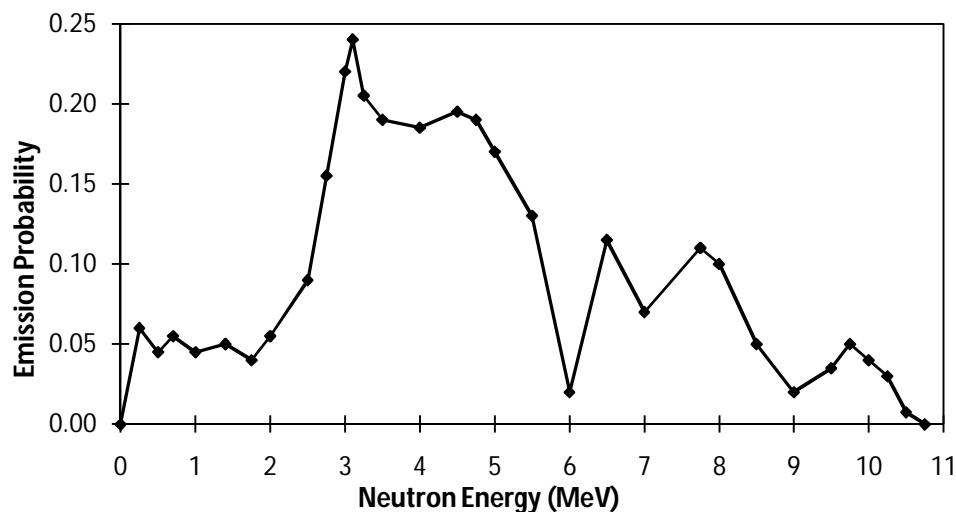
Fig. 2. Expected neutron energy spectrum of the Pu-Be source adapted from Kumar and Nagarajan (1977)

3. S&TSub Improvements

The S&TSub's fixed detector tube does not allow a wide variety of experiments to be performed. Detector position can only be adjusted radially with respect to the core. To enhance the experimental capability of the S&TSub a new detection system was created. Two 182.3 cm long acrylic tubes were fabricated with acrylic stoppers at the bottom to make them water proof and loaded with lead weights to counteract their buoyancy. A small ^{3}He neutron detector was outfitted with radial spacers to keep it centered while suspended by its data cable in each tube. Since the acrylic tubes have the same outer diameter as a fuel guide tube, and since the detectors can be positioned at any axial location within the tube, three dimensional neutron flux measurements of the S&TSub are now possible. Figure 3 shows a fully prepared movable detector tube ready for insertion into the S&TSub.

Fig. 3. Movable detector tube assembly. A. Cap detector is suspended from. B. Preset suspension locations. C. ^{3}He neutron detector. D. Lead weights. E. Acrylic stopper.

Table 3. S&TSub operating characteristics

Detector	Operating Voltage	LLD (V)	Window (ΔE)
1	1650 V	0.002	0.990
2	1493 V	0.002	0.990
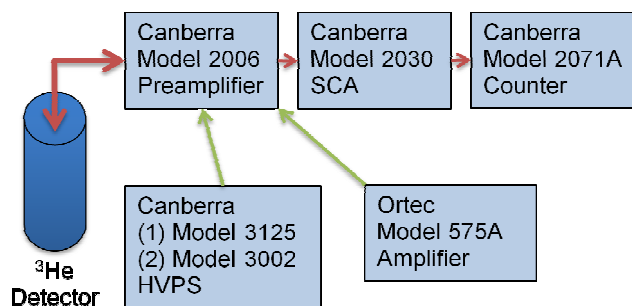
Fig. 4. S&TSub facility experimental setup. A different model high voltage power supply (HVPS) is used for each detector, though the other components are identical.
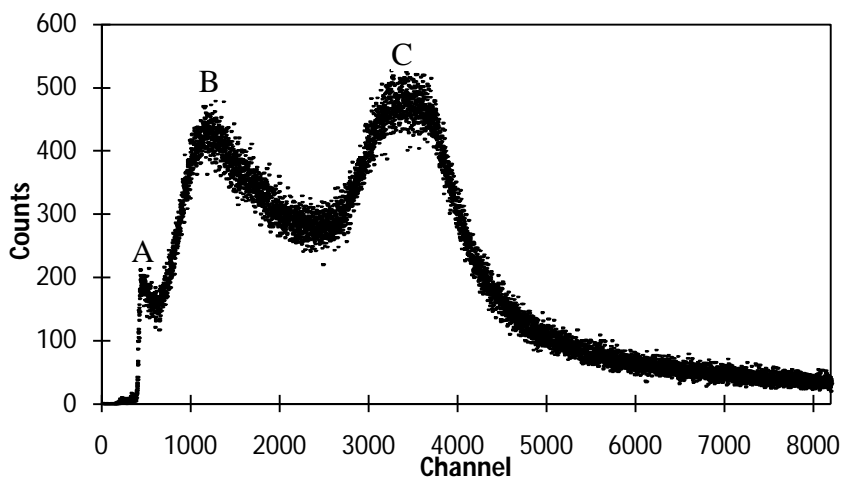
Fig. 5. ^{3}He detector pulse height spectrum, demonstrating the wall effect. A. ^{3}H escapes. B. Proton escapes. C. Neither product escapes.

3.1 ^{3}He Neutron Detector

The new detection system uses Canberra model 0.5NH1/1K ^{3}He neutron detector. This detector was chosen because of its high neutron sensitivity (0.5 c s^{-1} per n cm^{-2} s^{-1}) low gamma sensitivity and small active volume (1 cm long and 0.9 cm diameter) providing high spatial accuracy, ideal for flux mapping. Figure 4 shows the experimental

setup and Table 3 lists the system operating characteristics used for all of the experiments performed for this project.

Because neutrons are indirectly ionizing radiation they must create charged particles to be detected. In a ^{3}He detector thermal neutrons are counted after the ^{3}He(n,p)^{3}H reaction occurs. The amount of energy deposited in the detector depends on where this reaction occurs. If a neutron is absorbed near the detector wall it is possible for one of the reaction products to escape the detector without depositing any energy (Leake, 2005). This effect can be seen in Figure 5, which is pulse height spectrum collected using the new S&TSub detection system. Peak A corresponds to the escape of the proton, meaning only the triton deposits its energy in the detector. Peak B corresponds to the escape of the triton, meaning only the proton deposits its energy in the detector. Peak C is produced when neither the proton nor the triton escapes the detector.

3.2 Void Tube

The experimental setup for a void coefficient experiment was also created. 41 holes 0.6 cm in diameter were drilled 2.5 cm apart into a 182.3 cm acrylic tube starting 16 cm from the bottom of the tube. The holes are large enough for a balloon to be inserted and inflated, allowing a void to be deployed anywhere along the fuel length, and since the acrylic tube has the same outer diameter as the fuel guide tube a void can be inserted into any empty fuel position. Figure 6 shows the void tube with an inflated balloon.
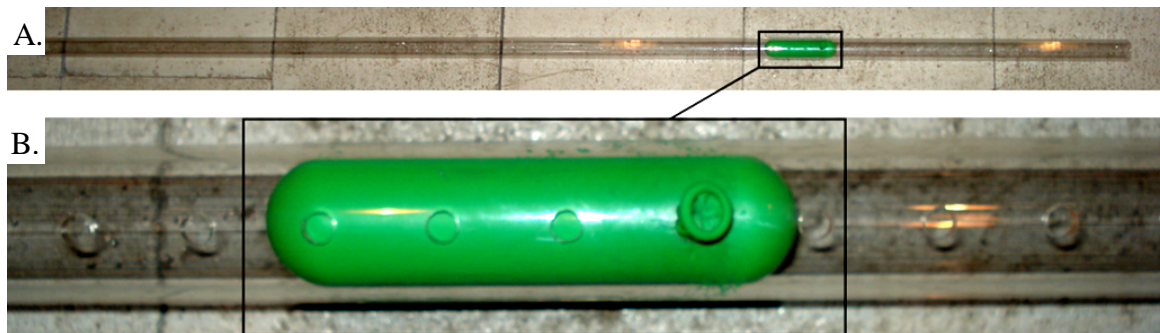
Fig. 6. A. Void tube ready for use in the S&TSub. B. Detail of void

3.3 Internet Accessibility

A Canberra Lynx Counting System provides limited internet access to the S&TSub for remote users. The Lynx system was installed as part of the Missouri S&T Internet Accessible Hot Cell Facility (Grant et al., 2011). Through the Lynx interface a detector can be turned on and off, counting can be started and stopped, and several settings can be adjusted such as coarse gain, fine gain, counting time, and applied voltage (Lynx, 2011). However, remote users can not adjust axial or radial detector location, void location, or fuel arrangement without assistance from reactor personnel. Figure 7 shows a measurement of the S&TSub power ramp as the neutron source was removed and reinserted. This data was acquired with the Lynx system.
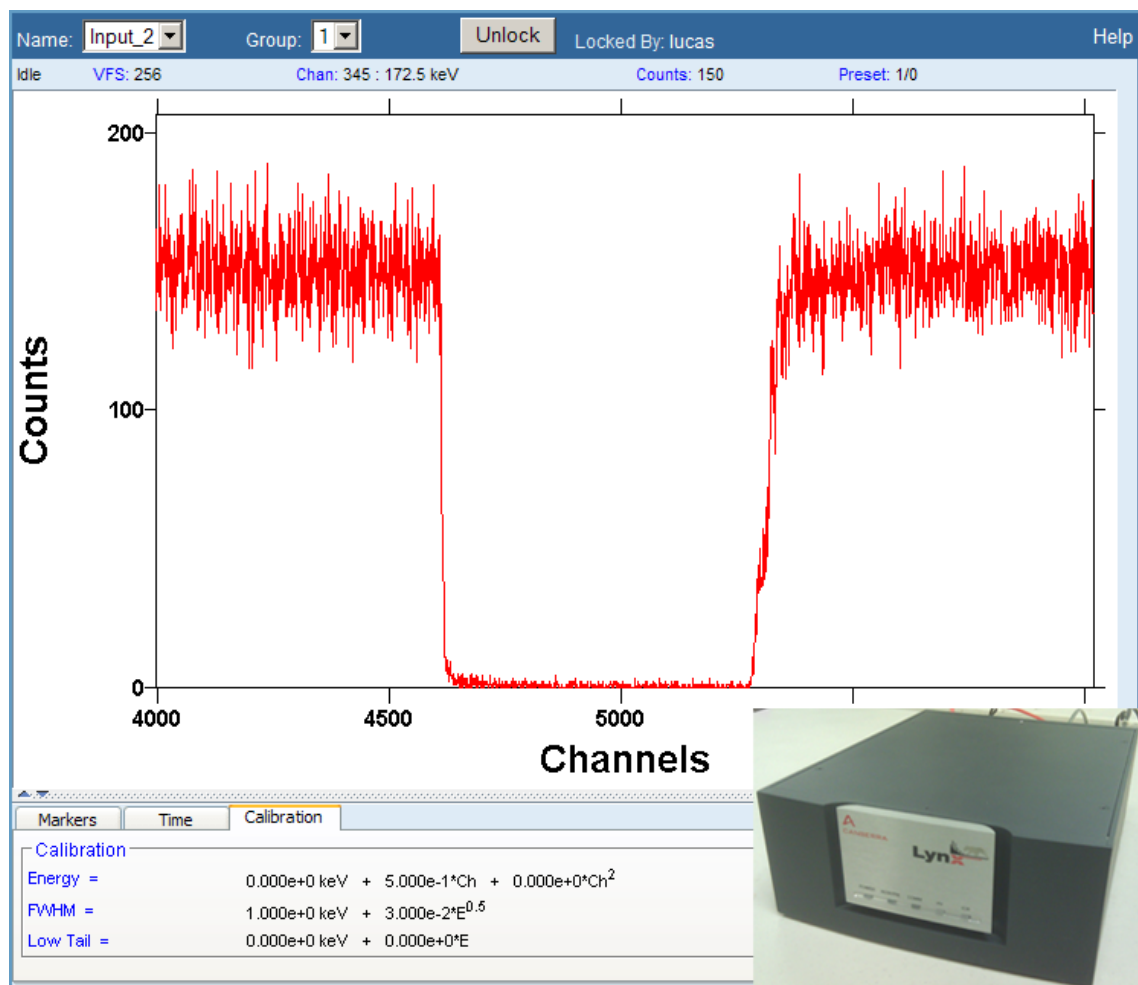
Fig. 7. S&TSub power ramp acquired with Lynx Digital Signal Analyzer (inset) demonstrating the Lynx user interface

4. MCNP Model Development and Validation

Monte Carlo N-Particle transport code is a useful tool for precisely modeling a reactor's geometry and simulating the paths neutrons will travel through and interact with materials. MCNP can compute data about the number of particles crossing a surface or absorbed by a material. It can also process this information to predict reactor characteristics such as the multiplication factor. An MCNP model of the S&TSub was created for this project to understand the current configuration of the facility and predict the effect of any changes to the configuration. The movable detector tubes and the void tube were also modeled so that the results of the simulation could be compared to experimental results for model validation. Each simulation was performed with fifty million particle histories so that no tally had more than 10% relative error. Figure 8A shows an overhead view of the S&TSub facility, while Figure 8B is a radial cross section from the MCNP model taken through the top grid plate and Figure 8C shows an axial cross section of the MCNP model taken through the center of the neutron source.

A.   B.   C.
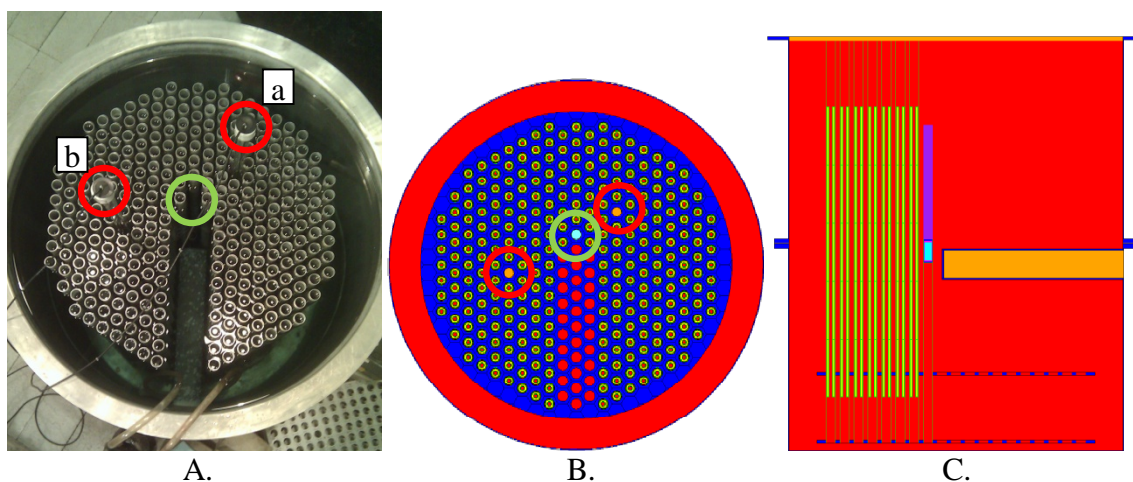
Fig. 8. A. Fully loaded S&TSub with each movable detector tube indicated by a red circle and the neutron source circled in green. B. Radial cross section of MCNP model through the top grid plate (27.5 cm from the tank bottom) C. Axial cross section of MCNP model through the center of the neutron source and the fixed detector tube.

4.1 Approach to Criticality

Though a subcritical assembly will never become critical, when a neutron source is present it will have a steady population of neutrons quantified by the multiplication rate (M) (Valente, 1963). M is determined by dividing the combined neutron flux from the source and fission by the flux from the source alone (Valente, 1963). Equation 2 shows a geometric series by neutron generation that can be used to calculate the multiplication rate based on the source activity (Q) and k_{eff} (Valente, 1963).

$$M = \frac{Q + Qk_{eff} + Qk_{eff}^2 + \cdots}{Q} \tag{2}$$

As the number of neutron generations becomes very large and k_{eff} is less than unity, M simplifies to equation 3 (Valente, 1963).

$$M = \frac{1}{1 - k_{eff}} \tag{3}$$

To determine k_{eff} experimentally, the multiplication rate can be approximated as the ratio of neutron count rates after a certain amount of fuel is loaded (R') and before any fuel was present (R_0) as seen in equation 4 (Valente, 1963).

$$M = \frac{R'}{R_0} \tag{4}$$

An equation to determine k_{eff} can be developed by combining equations 3 and 4.

$$k_{eff} = 1 - \frac{1}{M} \tag{5}$$

The 1/M approximation, as the above method is known, was used to determine k_{eff} for the S&TSub. To accomplish this, the movable detector tubes were placed in the positions where they are seen in Figure 8A. Fuel was loaded in concentric rings around the source, which was placed in the position nearest to the center of the assembly circled in green in Figure 8A. Eleven loads were required to add all the S&TSub fuel rods to the core. Neutron count rate measurements were taken as fuel was loaded into the S&TSub. For each measurement, counts were taken with both detectors in five axial locations such that the active volume of the detector was in line with the center of each fuel slug.

This experiment was simulated using MCNP. Rather than running a different simulation for each axial detector location, all five detector locations were combined into one tube and simulated simultaneously. Since the distance between detector locations is large compared to their active length, the tally results for a particular detector were

unaffected by the presence of additional simulated detectors in the tube. An F4 tally, which calculates fluence normalized per source particle (n cm^{-2} sp^{-1}), was applied to the active volume of each simulated detector, generating R_0 and R' for the 1/M approximation. MCNP has a more direct method of calculating the k_{eff}, the KCODE command. Using the KCODE command, MCNP approximates k_{eff} by estimating the number of fission neutrons produced per fission neutron started for a given generation. By repeating this process for thousands of generations MCNP arrives at a good approximation of a pile's multiplication factor (X-5 Monte Carlo Team, 2005). The KCODE command was also applied for every fuel load to provide an additional data point for comparison with experimental results.

In Figure 9 the results of the approach to criticality equations for the experimental measurements and for the MCNP tallies are plotted with the results of the KCODE simulation for both detector tubes and each detector location within the tube. The height of each detector location from the bottom of the tank (H) and the radial distance from the source tube to the movable detector tube (R) were measured. Also, the straight-line distance from the neutron source to the detector centroid (D) was calculated. This information is included with each plot in Figure 9.

It is clear from Figure 9 that detector location has an important effect on how closely the results from MCNP match experimental results and how closely the 1/M approximation for k_{eff} matches the KCODE results. The ability of the 1/M approximation to accurately predict k_{eff} depends on the ratio of source neutrons to fission neutrons. When the detector is far away from the source and most of the neutrons it reads are from fission, the 1/M approximation over-predicts k_{eff}. Conversely, when the detector is too close to the source and reads too many source neutrons the 1/M approximation under-predicts k_{eff}. However, when the right ratio of source and fission neutrons is read by the detector the 1/M approximation provides a good estimate of k_{eff}. This relationship is illustrated in Figure10, which compares the measured and simulated 1/M results from each detector to the KCODE results. This figure shows that detector locations a4, b3, and b4, which are between 27 and 36 cm from the neutron source deviate from KCODE by less than 10% whether simulated or measured.
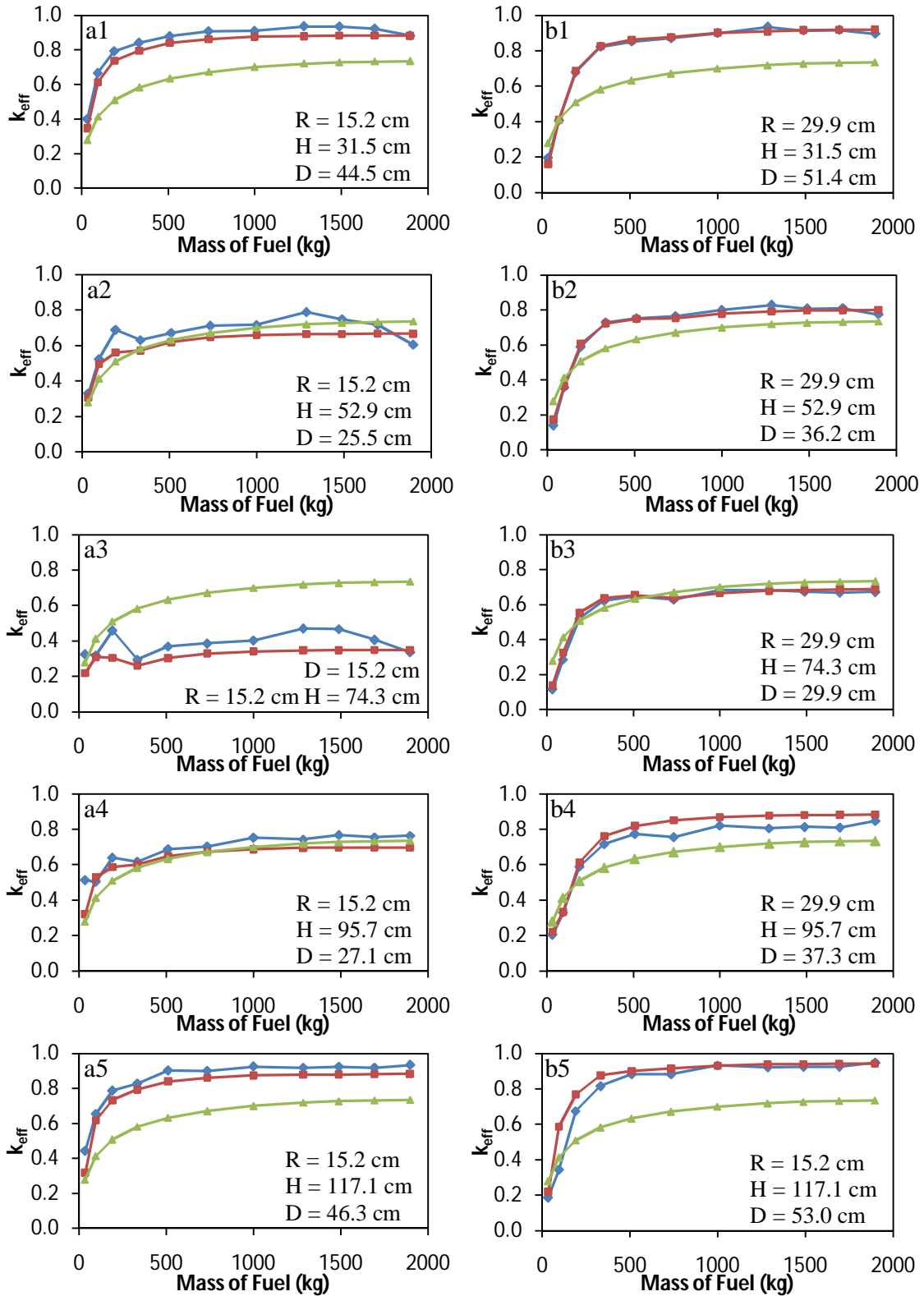
Fig. 9. Comparison of results for k_{eff}. ◆ 1/M approximation from measured values, ■ 1/M approximation from MCNP tallies, ▲ MCNP KCODE results. Radial (R) and axial (H) location is included with the distance from the detector to the neutron source (D).
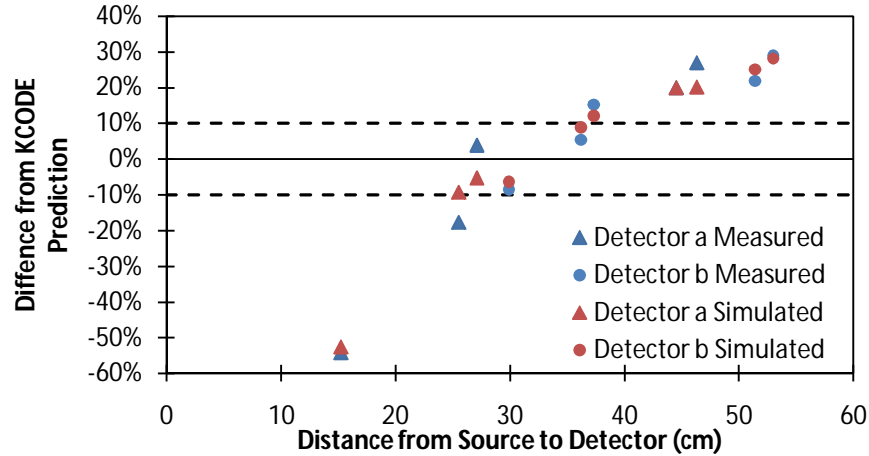
Fig. 10. Difference between KCODE and simulated and measured 1/M approximations for k_{eff} by location and detector for the fully loaded S&TSub

4.2 Axial Flux Profile

The next validation experiment performed was an axial flux measurement. One of the movable detector tubes was configured to take measurements at 21 different axial locations, and a corresponding model was built in MCNP. All detector locations were simulated simultaneously. The neutron fluence per source particle was tallied at each simulated detector location. Figure 11 shows the relevant geometry and Figure 12 shows a comparison of the measured and simulated data using this arrangement. The difference between the two curves is likely due to location measurement error.
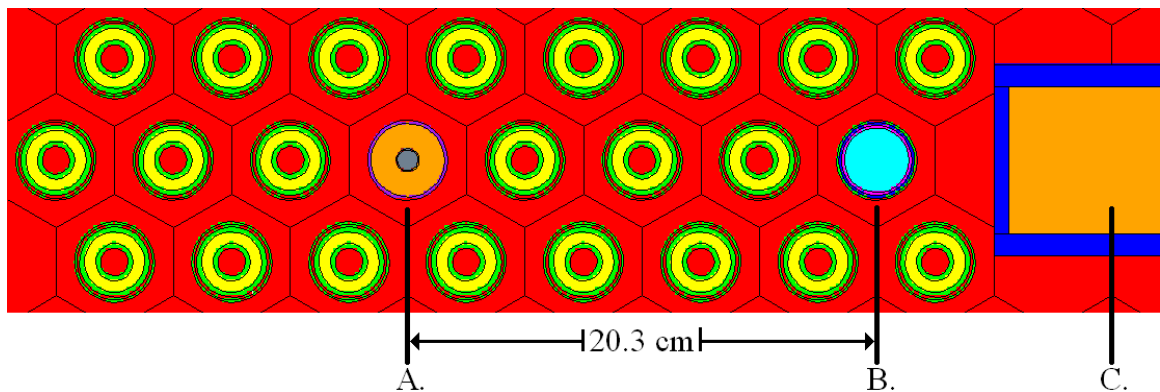
Fig. 11. Relevant geometry for the axial flux profile experiment. A. Movable detector tube. B. Pu-Be neutron source. C. Fixed detector tube
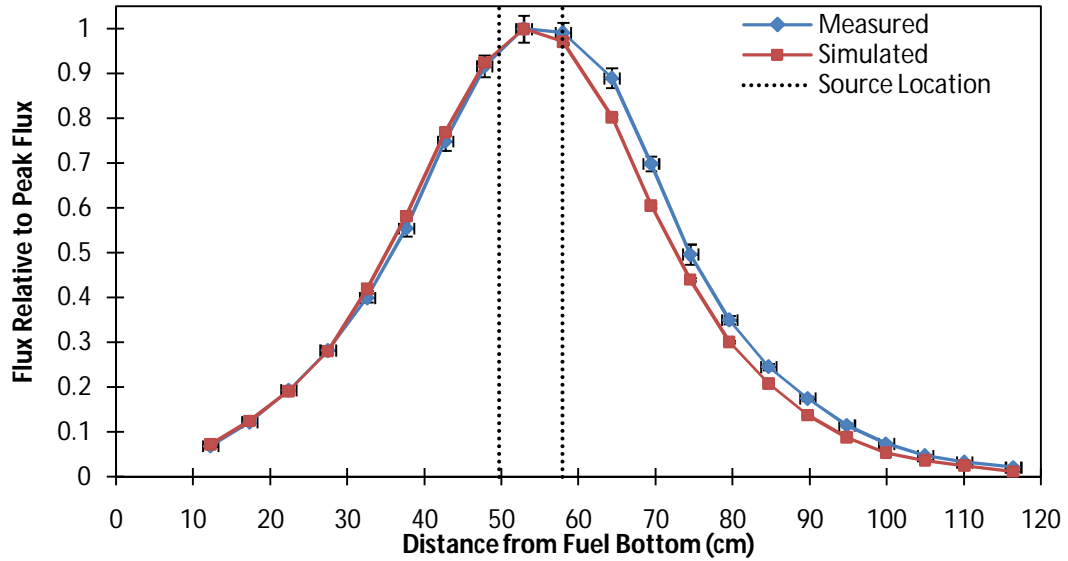
Fig. 12. Measured and simulated axial flux profiles

4.3 Void Effect

One final comparison was made between the MCNP model and the experimental results collected from the S&TSub. The void tube discussed in section 3.2 was prepared and inserted into the S&TSub according to the geometry depicted in Figure 13. Neutron count rate measurements were taken at the same 21 detector locations. The void was removed, though the acrylic tube remained in place, and the axial flux profile was measured again. The flux relative to the peak flux with the void in place was calculated for both data sets, and the results were plotted in Figure 14A. This experiment was simulated with MCNP and the relative flux tally results are plotted in Figure 14B.
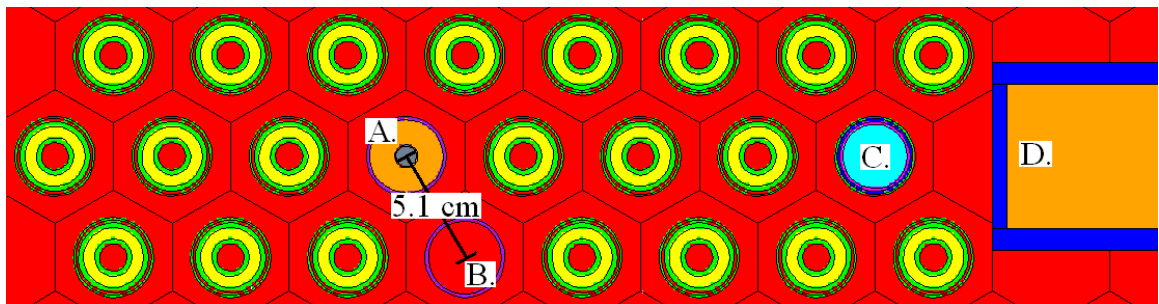
Fig. 13. Relevant geometry for the void tube experiment. A. Movable detector tube. B. Void tube. C. Neutron source. D. Fixed detector tube.
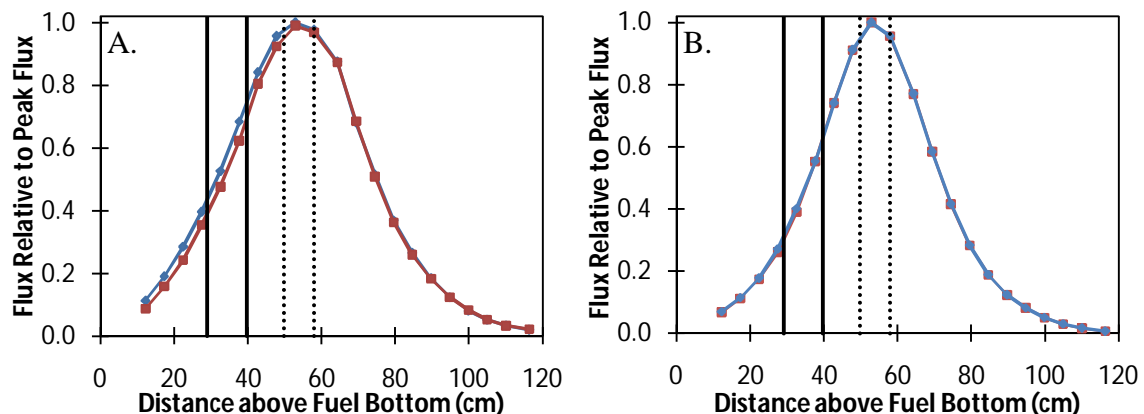
Fig. 14. Relative flux with void (—◆—) and without void (—■—). A. Experimentally measured values. B. MCNP Simulated values. The solid vertical line denotes the location of the void. The dotted vertical line denotes the source location.

Though it is possible to see the difference in flux between the measurements with the void and without the void, the difference is small, and the simulated results are indistinguishable. To better represent the change in the S&TSub flux characteristics in the presence of a void, the percent change after the void was added is plotted in Figure 15 for experimentally measured and simulated flux values. The MCNP model does not accurately predict the change that occurred in the experiment, but this could be due to the negligible impact the void had. Also, the void shrank in the cold water of the S&TSub meaning that the modeled void was larger than the actual void. This experiment should be repeated with a larger void that does not change size.
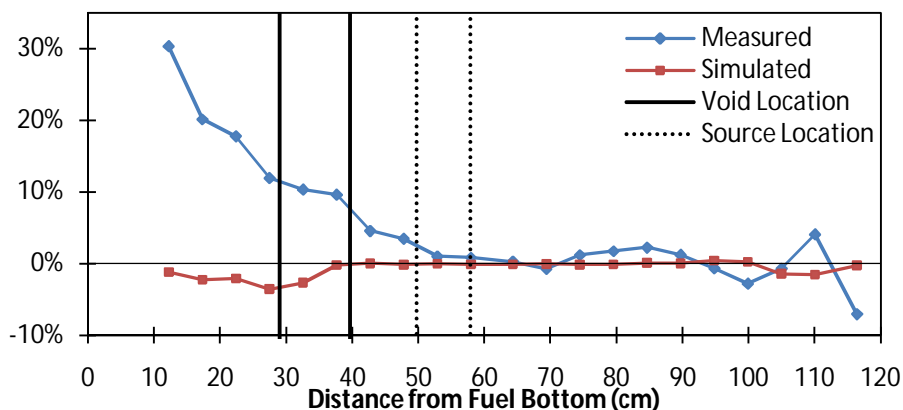
Fig. 15. Percent change in flux after the void was added for measured and simulated flux

5. Future Work: Removing the Fixed Detector Tube

The current design of S&TSub includes a fixed detector tube, which covers 31 lattice positions – including the center position. This arrangement makes the S&TSub more difficult to use. First, the symmetry is reduced. There is only one axis of symmetry, as seen in Figure 8, which means that to create a 3D flux map measurements must be taken in half of the fuel positions. Greater fuel symmetry would reduce the amount of time required for flux mapping by reducing the number of positions where flux needs to be measured. Another major problem with the fixed detector tube is that it extends beyond the center of the assembly. This changes the shape of the flux profile. The 31 empty lattice locations that are obstructed by the fixed detector tube dramatically increase neutron leakage from the core, reducing the magnitude of the neutron flux.

Not only does the fixed detector tube detrimentally impact the flux characteristics of the S&TSub it is also difficult to use for neutron measurements. There is very little flexibility in detector location, and though the detector can be placed in the center of the assembly radially, it is not possible to center it axially because the fixed detector tube does not cross the axial mid-plane of the S&TSub. Also, the neutron source must be placed as close to the detector tube as possible to maximize flux and optimize the flux profile, but the neutrons from the source mask the neutrons generated by fission, reducing the accuracy of the results. If the fixed detector tube were removed and the core were rearranged all of these issues could be eliminated.

5.1 Five Potential Load Patterns without the Fixed Detector Tube

To analyze the effect of removing the fixed detector tube, the MCNP model of the S&TSub was modified to remove the tube and five potential core loading patterns were considered. For each configuration the fuel was rearranged to maximize symmetry. The load patterns were compared to each other and the current load pattern based on the multiplication factor predicted by the KCODE command in MCNP. Figure 16 displays the current load pattern and the five potential load patterns that were analyzed, while the results of the simulations can be seen in Table 4.
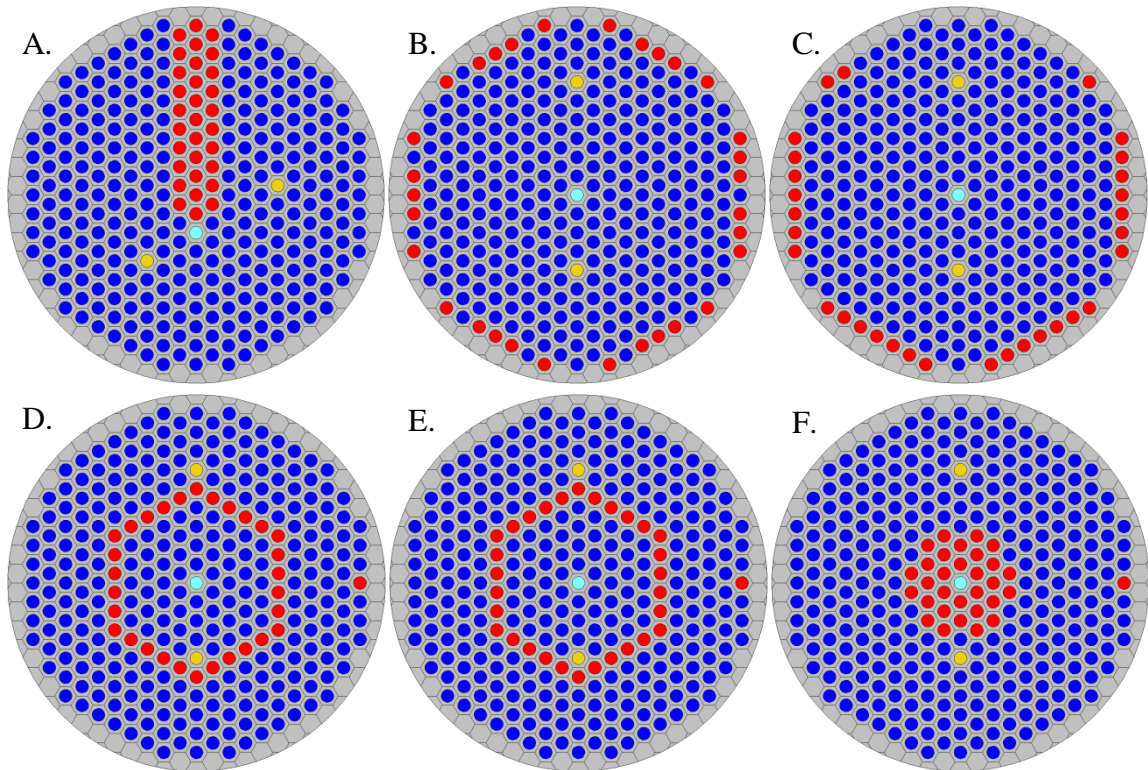
Fig. 16. S&TSub core configurations. A. Current configuration, with fixed detector tube. B. through F. Without-fixed-detector-tube configurations 1-5, respectively. Colors are assigned as follows: ● Fuel, ● Empty, ● Movable detector tube, ● Neutron source.

Table 4. Predicted k_{eff} for the current configuration and five potential configurations

	Current	1	2	3	4	5
k_{eff}	0.73481	0.76844	0.76884	0.76858	0.70554	0.71459
SD	8.080E-05	4.610E-05	4.613E-05	8.454E-05	7.761E-05	7.860E-05

5.2 Advantages of Removing the Fixed Detector Tube

Table 4 shows that by removing the fixed detector tube, centralizing the source, and redistributing the fuel symmetrically the multiplication factor can be increased from 0.73481±8.080E-05 to 0.76844±4.610E-05 if configuration 1 is applied. We can also conclude the fuel distribution in the outermost ring of fuel does not affect the improvement much. Furthermore, removing the fixed detector tube and reconfiguring the fuel would improve the magnitude and symmetry of the flux distribution. Evidence of
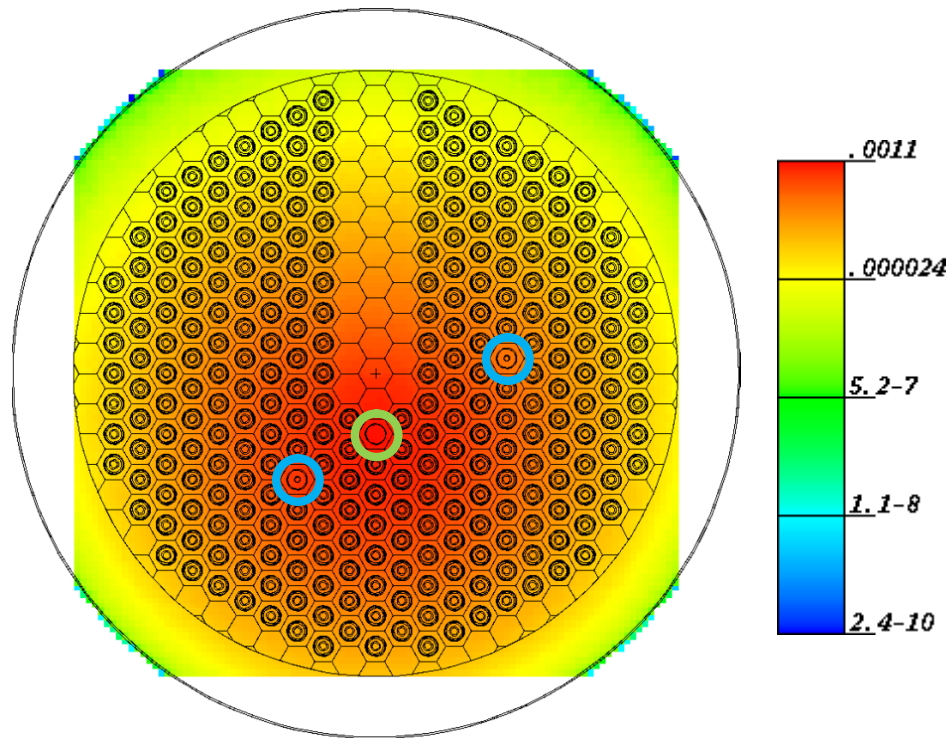
Fig. 17. Neutron flux distribution (n cm^{-2} sp^{-1}) 51.64 cm from the tank bottom for the current core configuration. Detectors are circled in blue. Source is circled in green.
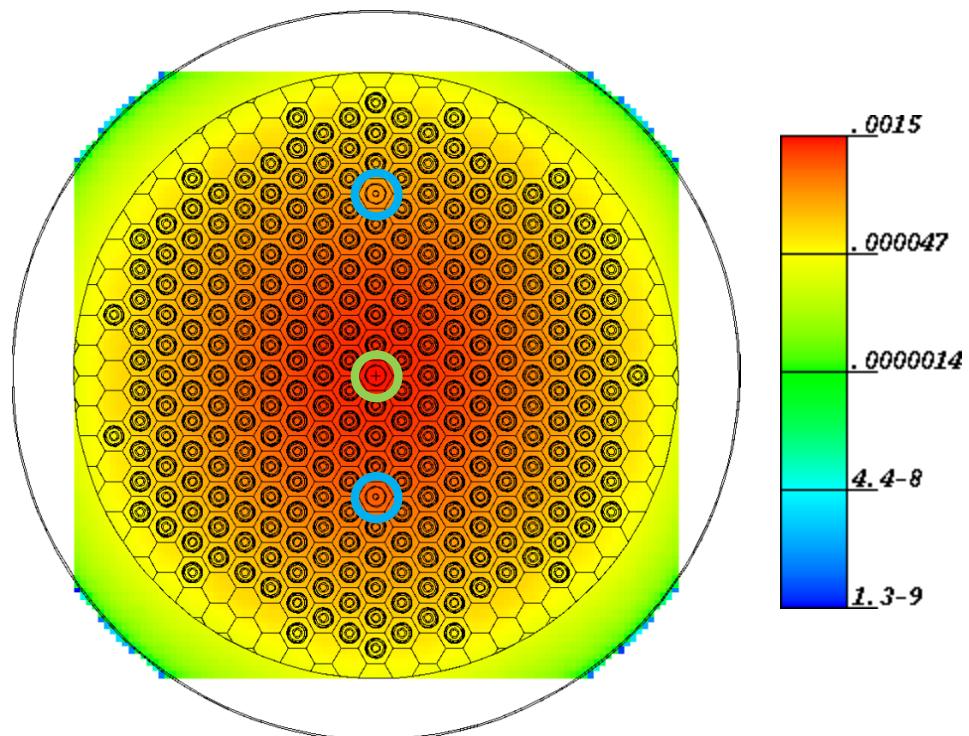
Fig. 18. Neutron flux distribution (n cm^{-2} sp^{-1}) 51.64 cm from the tank bottom for recommended configuration 1. Detectors are circled in blue. Source is circled in green.

this is shown in Figures 17 and 18, which show the radial flux distribution 51.64 cm from the tank bottom for the current core configuration and configuration 1 respectively. The more uniform flux distribution provided by redistributing the core according to configuration 1 would allow faster mapping of the core by making it easier to extrapolate measurements across the core. Another benefit of removing the fixed detector tube and redistributing the core would be an increase in neutron flux. MCNP predicts a 36% increase in peak neutron flux on this plane from 0.0011 n cm^{-2} s^{-1} to 0.0015 n cm^{-2} s^{-1}.

6. Conclusions

The Missouri University of Science and Technology Subcritical Assembly is once again fully loaded with fuel and operational. It has been upgraded with two movable detector tubes that allow several new experiments to be performed. These experiments include 3D flux mapping, void effects, and approach to criticality. With the help of a Lynx Digital Signal Analyzer limited internet accessible capabilities are available to distance users.

An MCNP model of the S&TSub was created to simulate the results of experiments and predict the effects of changes to the facility. The MCNP model was validated by comparing its results to a series of experimentally collected values. First an approach to criticality experiment to calculate k_{eff} was performed using the 1/M approximation. Measured and simulated values for k_{eff} from the 1/M approximation agreed very well, with a maximum difference of 10%. The 1/M approximation also agreed well with the KCODE predictions for detector locations between 27 cm and 36 cm from the neutron source. An axial flux profile measurement was also performed and simulated. With an average relative error of 12%, the MCNP model accurately predicts the experimentally measured results. Finally, a void effect experiment was performed and simulated. This simulation did not accurately predict the experimental results, probably because of the small impact of the void on neutron flux. The experiment should be redesigned and redone.

Using the validated MCNP model, predictions were made about the effect of removing the fixed detector tube from the S&TSub. The fixed detector tube is difficult to use and detrimental to the neutron flux characteristics. Based on MCNP simulations the

k_{eff} of the S&TSub would increase from 0.73481±8.080E-05 to 0.76844±4.61E-05 if configuration 1 were applied. Also, moving the neutron source into the center of the assembly would increase the neutron flux by 36% and distribute it more evenly allowing better extrapolation of measurements across the core. Future work should focus on removing the fixed detector tube, optimizing core loading, and verifying the MCNP model predictions.

References

Baum, E.M., Knox, H.D., Miller, T.R., 2002. Chart of the Nuclides, sixteenth ed. Knoll's Atomic Power Laboratory, Inc.

Grant, E.J., Mueller, G.E., Castaño, C., Kumar, A.S., Usman, S., 2011. Internet accessible hot cell with gamma spectroscopy at the Missouri S&T nuclear reactor. Nuclear Engineering and Design. In press.

Gunnink, R., Niday, J.B., Siemens, P.D., 1974. A system for plutonium analysis by gamma ray spectrometry part 1: techniques for analysis of solutions. Lawrence Livermore Laboratory Report UCRL-5 1577, Part 1.

Kumar, A., Nagarajan, P.S., 1977. Neutron spectra of [239]Pu-Be Sources. Nuclear Instruments and Methods. 140, 75-179.

Leake, J.W., Croft, S., McElroy, R.D., Lambert, K.P., 2005. Annual meeting of the INMM. <http://www.canberra.com/literature/13544.asp>. Accessed 29 March 2011.

Lynx Digital Signal Analyzer Data Sheet. <http://www.canberra.com/pdf/products/c38389-lynx-ss.pdf>. Accessed 29 March 2011.

Maldonado, G.I., Xoubi, N., Zhongxiang, Z., 2008. Enhancement of a subcritical experimental facility via MCNP simulations. Annals of Nuclear Energy. 35, 263-268.

Runnals, O.J.C., Boucher, R.R., 1956. Neutron yields from actinide-beryllium sources. Canadian J. Phys. 34, 949-958.

Tate R.E., Coffinberry A.S., 1958. Plutonium-beryllium neutron sources, their fabrication and neutron yield. Second United Nations International Conference on the Peaceful Uses of Atomic Energy.

Valente, F.A., 1963. A Manual of Experiments in Reactor Physics. Macmillan, New York.

X-5 Monte Carlo Team, 2005. MCNP – A General Monte Carlo N-Particle Transport Code, Version 5. LA-UR-03-1987. Los Alamos National Laboratory.

APPENDIX A

S&TSUB MCNP MODEL INPUT DECK

```
continue Subcritical Assembly - Water at or above guide tube
c **************************************************************************
c
c **************************************************************************
c
c Stainless Steel Tank with Lead Gasket
1    2 -7.92 -1 4 -10 11          imp:n=1 $ Top Flange
2    2 -7.92 -3 4 -11 12          imp:n=1 $ Top Tank Wall
3    2 -7.92 -2 4 -12 13          imp:n=1 $ Top Middle Flange
4    8 -11.34 -2 4 -13 14         imp:n=1 $ Lead Gasket
5    2 -7.92 -2 4 -14 15          imp:n=1 $ Bottom Middle Flange
6    2 -7.92 -3 4 -15 16 #22      imp:n=1 $ Bottom Tank Wall
7    2 -7.92 -3 -16 17            imp:n=1 $ Tank Bottom
8    7 -0.001225 -1 30 -9 10      imp:n=1 $ Air above tank and outside lattice
c
c Inside Stainless Steel Tank but Outside Lattice
10   7 -0.001225 -4 30 -10 32       imp:n=1 $ Air above water and below tank top
11   1 -1.00 -4 30 -32 16 #20 #21 #22 imp:n=1 $ Outside lattice below air
12   1 -1.00 -30 -36 16            imp:n=1 $ Below lattice
c
c Tank Detector Tube
20   2 -7.92 -20 21 22 -4         imp:n=1 $ Cylinder
21   2 -7.92 -21 22 -23           imp:n=1 $ Front
22   7 -0.001225 -21 23 -3        imp:n=1 $ Air Inside
c
c Universe 1 - Water and grid plate without hole
101 7 -0.001225 32               u=1 imp:n=1 $ Air above water
102 1 -1.00 -32 33               u=1 imp:n=1 $ Water above grid plate
103 2 -7.92 -33 34               u=1 imp:n=1 $ Top grid plate (no hole)
104 1 -1.00 -34 35               u=1 imp:n=1 $ Water between grid plates
105 2 -7.92 -35                  u=1 imp:n=1 $ Bottom grid plate (no hole)
c
c Universe 2 - Water and grid plate with hole
201 like 101 but u=2                     $ Air above water
202 like 102 but u=2                     $ Water above top grid plate
203 2 -7.92 -33 34 31            u=2 imp:n=1 $ Top grid plate (w/ hole)
204 1 -1.00 -33 34 -31           u=2 imp:n=1 $ Water in top grid plate hole
205 like 104 but u=2                     $ Water between grid plates
206 2 -7.92 -35 31               u=2 imp:n=1 $ Bottom grid plate (w/ hole)
207 1 -1.00 -35 -31              u=2 imp:n=1 $ Water in bottom grid plate hole
c
c Universe 3 - Fuel
301 like 101 but u=3                     $ Air above water
302 1 -1.00 -32 51               u=3 imp:n=1 $ Water above guide tube
303 1 -1.00 -51 33 31            u=3 imp:n=1 $ Outside tube above grid plate
304 1 -1.00 -34 35 31            u=3 imp:n=1 $ Outside tube btwn grid plates
305 1 -1.00 -51 48 -50           u=3 imp:n=1 $ Inside guide tube above fuel
306 1 -1.00 -48 47 -50 40        u=3 imp:n=1 $ Inside guide tube outside fuel
307 1 -1.00 -48 47 -43           u=3 imp:n=1 $ Inside fuel slugs
308 1 -1.00 -47 -50              u=3 imp:n=1 $ Inside guide tube below fuel
310 4 -2.712 -51 36 -31 50       u=3 imp:n=1 $ Guide tube
311 like 203 but u=3                      $ Top grid plate (w/ hole)
312 like 206 but u=3                      $ Bottom grid plate (w/ hole)
320 4 -2.712 -44 45 -40 43       u=3 imp:n=1 $ Clad top cap     1
321 4 -2.712 -45 46 -40 41       u=3 imp:n=1 $ Clad outer wall 1
322 4 -2.712 -45 46 -42 43       u=3 imp:n=1 $ Clad inner wall 1
323 4 -2.712 -46 47 -40 43       u=3 imp:n=1 $ Clad bottom cap 1
324 3 -19.1  -45 46 -41 42       u=3 imp:n=1 $ Fuel Slug       1
330 like 320 but trcl=10                  $ Clad top cap     2
331 like 321 but trcl=10                  $ Clad outer wall 2
332 like 322 but trcl=10                  $ Clad inner wall 2
333 like 323 but trcl=10                  $ Clad bottom cap 2
334 like 324 but trcl=10                  $ Fuel Slug       2
340 like 320 but trcl=11                  $ Clad top cap     3
341 like 321 but trcl=11                  $ Clad outer wall 3
342 like 322 but trcl=11                  $ Clad inner wall 3
343 like 323 but trcl=11                  $ Clad bottom cap 3
```

```
344 like 324 but trcl=11                        $ Fuel Slug        3
350 like 320 but trcl=12                        $ Clad top cap     4
351 like 321 but trcl=12                        $ Clad outer wall 4
352 like 322 but trcl=12                        $ Clad inner wall 4
353 like 323 but trcl=12                        $ Clad bottom cap 4
354 like 324 but trcl=12                        $ Fuel Slug        4
360 like 320 but trcl=13                        $ Clad top cap     5
361 like 321 but trcl=13                        $ Clad outer wall 5
362 like 322 but trcl=13                        $ Clad inner wall 5
363 like 323 but trcl=13                        $ Clad bottom cap 5
364 like 324 but trcl=13                        $ Fuel Slug        5
c
c Universe 4 - Detector Tube
401 7 -0.001225 31 32           u=4 imp:n=1 $ Air above water outside tube
402 1 -1.00 31 -32 33           u=4 imp:n=1 $ Water above grid outside tube
403 like 203 but u=4                        $ Top grid plate w/ hole
404 like 304 but u=4                        $ Water between grid plates
405 like 206 but u=4                        $ Bottom grid plate w/ hole
411 9 -1.18 -31 60 -9 35        u=4 imp:n=1 $ Acrylic tube
412 9 -1.18 -60 -71             u=4 imp:n=1 $ Acrylic stopper at bottom of tube
413 1 -1.00 -31 60 -35          u=4 imp:n=1 $ Water inside grid outside stopper
414 7 -0.001225 -60 -9 70       u=4 imp:n=1 $ Air above top detector postion
415 7 -0.001225 -60 61 -70 63   u=4 imp:n=1 $ Air between detector wall and tube
416 7 -0.001225 -60 -63 72      u=4 imp:n=1 $ Air below detector above Pb/air mix
417 12 8.077E-03 -60 71 -72     u=4 imp:n=1 $ Pb/air mix above stopper
421 10 -8.84 -61 62 -68 63      u=4 imp:n=1 $ Monel Detector Wall    1
422 10 -8.84 -62 -68 67         u=4 imp:n=1 $ Monel Detector Top     1
423 10 -8.84 -62 -64 63         u=4 imp:n=1 $ Monel Detector Bottom  1
424 7 -0.001225 -62 -67 66      u=4 imp:n=1 $ Air above Detector Gas 1
425 11 2.472E-4 -62 -66 65      u=4 imp:n=1 $ Detector Gas           1
426 7 -0.001225 -62 -65 64      u=4 imp:n=1 $ Air below Detector Gas 1
427 7 -0.001225 -61 68 -69      u=4 imp:n=1 $ Air between Detectors  1&2
431 like 421 but trcl=42                    $ Monel Detector Wall    2
432 like 422 but trcl=42                    $ Monel Detector Top     2
433 like 423 but trcl=42                    $ Monel Detector Bottom  2
434 like 424 but trcl=42                    $ Air above Detector Gas 2
435 like 425 but trcl=42                    $ Detector Gas           2
436 like 426 but trcl=42                    $ Air below Detector Gas 2
437 like 427 but trcl=42                    $ Air between Detectors  2&3
441 like 421 but trcl=43                    $ Monel Detector Wall    3
442 like 422 but trcl=43                    $ Monel Detector Top     3
443 like 423 but trcl=43                    $ Monel Detector Bottom  3
444 like 424 but trcl=43                    $ Air above Detector Gas 3
445 like 425 but trcl=43                    $ Detector Gas           3
446 like 426 but trcl=43                    $ Air below Detector Gas 3
447 like 427 but trcl=43                    $ Air between Detectors  3&4
451 like 421 but trcl=44                    $ Monel Detector Wall    4
452 like 422 but trcl=44                    $ Monel Detector Top     4
453 like 423 but trcl=44                    $ Monel Detector Bottom  4
454 like 424 but trcl=44                    $ Air above Detector Gas 4
455 like 425 but trcl=44                    $ Detector Gas           4
456 like 426 but trcl=44                    $ Air below Detector Gas 4
457 like 427 but trcl=44                    $ Air between Detectors  4&5
461 like 421 but trcl=45                    $ Monel Detector Wall    5
462 like 422 but trcl=45                    $ Monel Detector Top     5
463 like 423 but trcl=45                    $ Monel Detector Bottom  5
464 like 424 but trcl=45                    $ Air above Detector Gas 5
465 like 425 but trcl=45                    $ Detector Gas           5
466 like 426 but trcl=45                    $ Air below Detector Gas 5
c
c Universe 5 - Source and Source Holder
500 like 101 but u=5                        $ Air above water
501 1 -1.00 -32 90              u=5 imp:n=1 $ Below air, above holder
502 1 -1.00 31 -90 33           u=5 imp:n=1 $ Outside holder, above grid plate
503 like 203 but u=5                        $ Top grid plate
504 like 304 but u=5                        $ Water between grid plates
505 like 206 but u=5                        $ Bottom grid plate
```

```
506 9 -1.18 -31 -90 83        u=5 imp:n=1 $ Acrylic source holder rod
507 4 -2.712 -31 82 -83       u=5 imp:n=1 $ Aluminum guide tube
508 4 -2.712 -82 -88 89       u=5 imp:n=1 $ Bottom of source holder cup
509 1 -1.00 -82 -89           u=5 imp:n=1 $ Water below source holder cup
511 2 -7.92 -82 -83 84        u=5 imp:n=1 $ Top of SS clad
512 2 -7.92 -82 81 -84 87     u=5 imp:n=1 $ Wall of SS clad
513 2 -7.92 -82 -87 88        u=5 imp:n=1 $ Bottom of SS clad
521 6 -16.69 -81 -84 85       u=5 imp:n=1 $ Top of Tantalum clad
522 6 -16.69 -81 80 -85 86    u=5 imp:n=1 $ Wall of Tantalum clad
523 6 -16.69 -81 -86 87       u=5 imp:n=1 $ Bottom of Tantalum clad
531 5 -2.9 -80 -85 86         u=5 imp:n=1 $ PuBe
c
c Universe 6 - Detector Tube
601 7 -0.001225 31 32         u=6 imp:n=1 $ Air above water outside tube
602 1 -1.00 31 -32 33         u=6 imp:n=1 $ Water above grid outside tube
603 like 203 but u=6                     $ Top grid plate w/ hole
604 like 304 but u=6                     $ Water between grid plates
605 like 206 but u=6                     $ Bottom grid plate w/ hole
611 9 -1.18 -31 60 -9 35      u=6 imp:n=1 $ Acrylic tube
612 9 -1.18 -60 -99           u=6 imp:n=1 $ Acrylic stopper at bottom of tube
613 1 -1.00 -31 60 -35        u=6 imp:n=1 $ Water inside grid outside stopper
614 7 -0.001225 -60 -9 98     u=6 imp:n=1 $ Air above Detector 6.5
615 7 -0.001225 -60 61 -98 91 u=6 imp:n=1 $ Air between detector wall and tube
616 7 -0.001225 -60 -91 100   u=6 imp:n=1 $ Air below detectors above Pb/air
617 12 8.077E-03 -60 99 -100  u=6 imp:n=1 $ Pb/air mix above stopper
621 10 -8.84 -61 62 -96 91    u=6 imp:n=1 $ Monel Detector Wall    1
622 10 -8.84 -62 -96 95       u=6 imp:n=1 $ Monel Detector Top     1
623 10 -8.84 -62 -92 91       u=6 imp:n=1 $ Monel Detector Bottom  1
624 7 -0.001225 -62 -95 94    u=6 imp:n=1 $ Air above Detector Gas 1
625 11 2.472E-4 -62 -94 93    u=6 imp:n=1 $ Detector Gas           1
626 7 -0.001225 -62 -93 92    u=6 imp:n=1 $ Air below Detector Gas 1
627 7 -0.001225 -61 -97 96    u=6 imp:n=1 $ Air between Detectors  1&2
631 like 621 but trcl=42                 $ Monel Detector Wall    2
632 like 622 but trcl=42                 $ Monel Detector Top     2
633 like 623 but trcl=42                 $ Monel Detector Bottom  2
634 like 624 but trcl=42                 $ Air above Detector Gas 2
635 like 625 but trcl=42                 $ Detector Gas           2
636 like 626 but trcl=42                 $ Air below Detector Gas 2
637 like 627 but trcl=42                 $ Air between Detectors  2&3
641 like 621 but trcl=43                 $ Monel Detector Wall    3
642 like 622 but trcl=43                 $ Monel Detector Top     3
643 like 623 but trcl=43                 $ Monel Detector Bottom  3
644 like 624 but trcl=43                 $ Air above Detector Gas 3
645 like 625 but trcl=43                 $ Detector Gas           3
646 like 626 but trcl=43                 $ Air below Detector Gas 3
647 like 627 but trcl=43                 $ Air between Detectors  3&4
651 like 621 but trcl=44                 $ Monel Detector Wall    4
652 like 622 but trcl=44                 $ Monel Detector Top     4
653 like 623 but trcl=44                 $ Monel Detector Bottom  4
654 like 624 but trcl=44                 $ Air above Detector Gas 4
655 like 625 but trcl=44                 $ Detector Gas           4
656 like 626 but trcl=44                 $ Air below Detector Gas 4
657 like 627 but trcl=44                 $ Air between Detectors  4&5
661 like 621 but trcl=45                 $ Monel Detector Wall    5
662 like 622 but trcl=45                 $ Monel Detector Top     5
663 like 623 but trcl=45                 $ Monel Detector Bottom  5
664 like 624 but trcl=45                 $ Air above Detector Gas 5
665 like 625 but trcl=45                 $ Detector Gas           5
666 like 626 but trcl=45                 $ Air below Detector Gas 5
c
c Universe 9 - Lattice
700 0 -37 lat=2 u=9 imp:n=1
    fill=-12:12 -12:12 0:0
     1 1 1 1 1 1 1 1 1 1 1 1 1 1 1 1 1 1 1 1 1 1 1 1 1
      1 1 1 1 1 1 1 1 1 1 1 1 1 1 1 1 1 1 1 1 1 1 1 1 1
       1 1 1 1 1 1 1 1 1 1 1 1 1 1 3 3 3 3 3 3 3 3 1 1 1 1
        1 1 1 1 1 1 1 1 1 1 1 1 1 3 3 3 3 3 3 3 3 3 3 1 1 1
```

```
                1 1 1 1 1 1 1 1 1 1 3 3 3 3 3 3 3 3 3 3 3 3 3 3 3 1 1
                 1 1 1 1 1 1 1 1 1 3 3 3 3 3 3 3 3 3 3 3 3 3 3 3 1 1
                  1 1 1 1 1 1 1 1 3 3 3 3 3 3 3 3 3 3 3 3 3 3 3 1 1
                   1 1 1 1 1 1 1 3 3 3 3 3 3 3 3 3 3 3 3 3 3 3 1 1
                    1 1 1 1 1 1 3 3 3 3 3 3 3 3 3 3 3 3 3 3 3 1 1
                     1 1 1 1 1 3 3 3 3 3 4 3 3 3 3 3 3 3 3 3 3 3 3 1 1
                      1 1 1 1 3 3 3 3 3 3 3 3 3 3 3 3 3 3 3 3 3 1 1
                       1 1 1 1 3 3 3 3 3 3 3 3 2 2 2 2 2 2 2 2 2 1 1 1   $ det tube
                        1 1 1 3 3 3 3 3 3 3 3 5 2 2 2 2 2 2 2 2 2 2 1 1 1  $ det tube
                         1 1 1 3 3 3 3 3 3 3 3 2 2 2 2 2 2 2 2 2 2 1 1 1 1 $ det tube
                          1 1 3 3 3 3 3 3 3 3 3 3 3 3 3 3 3 3 3 3 1 1 1 1
                           1 1 3 3 3 3 3 3 3 3 3 3 3 3 3 3 3 3 3 1 1 1 1 1
                            1 1 3 3 3 3 3 3 3 3 3 3 3 3 3 3 3 3 1 1 1 1 1 1
                             1 1 3 3 3 3 3 3 3 6 3 3 3 3 3 3 3 1 1 1 1 1 1 1
                              1 1 3 3 3 3 3 3 3 3 3 3 3 3 3 1 1 1 1 1 1 1 1
                               1 1 3 3 3 3 3 3 3 3 3 3 3 3 3 1 1 1 1 1 1 1 1 1 1
                                1 1 3 3 3 3 3 3 3 3 3 3 3 3 1 1 1 1 1 1 1 1 1 1
                                 1 1 1 3 3 3 3 3 3 3 3 3 3 1 1 1 1 1 1 1 1 1 1 1 1
                                  1 1 1 1 3 3 3 3 3 3 3 3 1 1 1 1 1 1 1 1 1 1 1 1 1
                                   1 1 1 1 1 1 1 1 1 1 1 1 1 1 1 1 1 1 1 1 1 1 1 1 1
                                    1 1 1 1 1 1 1 1 1 1 1 1 1 1 1 1 1 1 1 1 1 1 1 1 1 1
c                                            S   C
c S=source C=Center
c
800 0 -9 36 -30 #20 #21 #22 fill=9 imp:n=1
c Void
900 0 9:(1 -9 10):(1 -10 11):(3 -11 12):(2 -12 15):(3 -15 17):-17 imp:n=0
c
c ****************************************************************************

c ****************************************************************************
c
c Tank Surfaces
1    cz   68.8578125   $ Top Flange Radius
2    cz   66.41211     $ Middle Flange/Lead Gasket Radius
3    cz   61.23686     $ Tank OR
4    cz   60.96        $ Tank IR
9    pz   186.21375    $ Top of air above tank
10   pz   152.4        $ Top of Tank
11   pz   151.12314    $ Bottom of Top Flange
12   pz   77.9145      $ Top of Middle Flange
13   pz   76.438125    $ Top of Lead Gasket
14   pz   76.2         $ Bottom of Lead Gasket
15   pz   74.422       $ Bottom of Middle Flange
16   pz   0            $ Bottom of Inside of Tank
17   pz   -0.27686     $ Bottom of Outside of Tank
c
c Tank Detector Tube Surfaces
20   c/y  0 68.58 5.715 $ OD
21   c/y  0 68.58 5.08  $ ID
22   py   -5.08        $ Outside of front
23   py   -4.445       $ Inside of front
c
c Lattice Definitions
30   cz   50.8         $ Outside of Lattice Region (Grid Plate Radius)
31   cz   1.7399       $ Grid Plate Hole Radius
32 1 pz   150.8761     $ Top of water (shift up with tr1)
33   pz   28.575       $ Top of Top Grid Plate
34   pz   27.305       $ Bottom of Top Grid Plate
35   pz   3.33375      $ Top of Bottom Grid Plate (S36=0)
36   pz   2.54         $ Bottom of Lattice (Bottom of Bottom Grid Plate)
37   rhp  0 0 2.54 0  0 186.21375  0 2.54 0 $ Hexagonal prism lattice element
c
c Bottom Fuel Slug Surfaces
c Use transforms 10-13 to generate other slugs
40   cz   1.524        $ Clad OR
41   cz   1.3081       $ Fuel OR
```

```
42    cz    0.8128        $ Fuel IR
43    cz    0.5969        $ Clad IR
44    pz    40.94         $ Clad Top
45    pz    40.7241       $ Fuel Top
46    pz    19.7559       $ Fuel Bottom
47    pz    19.54         $ Clad Bottom
48    pz   126.54         $ Clad Top on 5th fuel slug from bottom
c
c Guide Tube Surfaces
c Guide tube OR is equal to grid plate hole radius (surface 31)
c Bottom plane of guide tube is bottom of bottom grid plate (surface 35)
50    cz    1.64465       $ Guide tube IR
51    pz  150.876         $ Guide tube height
c
c Detector and Acrylic Tube Surfaces
c Acrylic tube OR is equal to grid plate hole radius (surface 31)
c Top plane of acrylic tube is top of air above tank (surface 9)
c Bottom plane of acrylic tube is top of bottom grid plate (surface 35)
60    cz    1.5875        $ Acrylic tube IR
61    cz    0.5           $ Detector Wall OR
62    cz    0.45          $ Detector Wall IR
63    pz    28.575        $ Detector 4.1 Wall Bottom outside
64    pz    28.625        $ Detector 4.1 Wall Bottom inside
65    pz    30.975        $ Detector 4.1 Bottom of He3 Detector Gas
66    pz    31.975        $ Detector 4.1 Top of He3 Gas
67    pz    38.925        $ Detector 4.1 Wall Top inside
68    pz    38.975        $ Detector 4.1 Wall Top outside
69    pz    50.00625      $ Top of air between Detectors 4.1 and 4.2
70    pz   124.7          $ Bottom of air above Detector 4.5
71    pz    7.9375        $ Top of acrylic stopper inside acrylic rod 4
72    pz    25.55875      $ Top of Pb/air mix in bottom of acrylic tube 4
c
91    pz    28.73375      $ Detector 6.1 Wall Bottom outside
92    pz    28.78375      $ Detector 6.1 Wall Bottom inside
93    pz    31.13375      $ Detector 6.1 Bottom of He3 Detector Gas
94    pz    32.13375      $ Detector 6.1 Top of He3 Gas
95    pz    39.08375      $ Detector 6.1 Wall Top inside
96    pz    39.13375      $ Detector 6.1 Wall Top outside
97    pz    50.165        $ Top of air between Detectors 6.1 and 6.2
98    pz   124.85875      $ Bottom of air above Detector 6.5
99    pz    8.09625       $ Top of acrylic stopper inside acrylic rod 6
100   pz    24.60625      $ Top of Pb/air mix in bottom of acrylic tube 6
c
c Source Surfaces
c Source guide tube OR is equal to grid plate hole radius (surface 31)
80    cz    1.397         $ PuBe OR
81    cz    1.5185        $ Tantanlum clad OR
82    cz    1.64          $ SS clad OR
83    pz    77.44077      $ Top of SS clad
84    pz    76.99627      $ Top of Tantalum Clad
85    pz    76.55177      $ Top of PuBe
86    pz    70.15097      $ Bottom of PuBe
87    pz    69.70647      $ Bottom of Tantalum clad
88    pz    69.26197      $ Bottom of SS clad
89    pz    69.16037      $ Bottom of cup source rests in
90    pz   135.53565      $ Top of acrylic source holder rod
c
c ****************************************************************************

c ****************************************************************************
c
c Transforms
tr1  0 0 0          $ Shift top of water above guide tube (surface 32)
c
tr10 0 0 21.4       $ 2nd fuel slug from bottom
tr11 0 0 42.8       $ 3rd fuel slug from bottom
tr12 0 0 64.2       $ 4th fuel slug from bottom
```

```
tr13 0 0 85.6      $ 5th fuel slug from bottom
c
tr42 0 0 21.43125 $ detector position 2
tr43 0 0 42.8625  $ detector position 3
tr44 0 0 64.29375 $ detector position 4
tr45 0 0 85.725   $ detector position 5
c
c Materials
c
m1   1001.66c   2.0         $ water
     8016.66c   1.0         $ 1.0 g/cc
mt1  lwtr.01t
c
m2   24050.66c  -0.8781     $ SS304
     24052.66c -16.9327     $ 7.92 g/cc
     24053.66c  -1.9200
     24054.66c  -0.4779
     25055.66c  -2.0133
     26054.66c  -4.0229
     26056.66c -63.1511
     26057.66c  -1.4584
     26058.66c  -0.1941
     28058.66c  -6.0938
     28060.66c  -2.3473
     28061.66c  -0.1020
     28062.66c  -0.3253
     28064.66c  -0.0829
c
m3   92238.66c -99.2745     $ natural uranium
     92235.66c  -0.7200     $ 19.1 g/cc
c
m4   13027.66c -97.8233     $ Aluminum 6061
     14028.66c  -0.6140     $ 2.712 g/cc
     14029.66c  -0.0312
     14030.66c  -0.0206
     12000.66c  -1.0536
     26054.66c  -0.0133
     26056.66c  -0.2093
     26057.66c  -0.0048
     26058.66c  -0.0006
     24050.66c  -0.0049
     24052.66c  -0.0939
     24053.66c  -0.0106
     24054.66c  -0.0026
     29063.66c  -0.0811
     29065.66c  -0.0362
c
m5   94239.66c -66.93       $ PuBe
     4009.66c -33.07        $ 2.9 g/cc
c
m6   73181.66c  -1.0        $ Tantalum
c                            16.69 g/cc
c
m7   7014.60c  -0.755636    $ Air
     8016.66c  -0.231475    $ 0.001225 g/cc
     18000.59c -0.012889
c
m8   82206.66c -24.1        $ Pb
     82207.66c -22.1        $ 11.34 g/cc
     82208.66c -52.4
c
m9   1001.66c   8.0         $ Acrylic
     8016.66c   2.0         $ 1.18 g/cc
     12000.66c  5.0
c
m10  28058.66c  0.507424    $ Monel
     28060.66c  0.26223     $ 8.84 g/cc
```

```
      28061.66c   0.0114
      28062.66c   0.03634
      28064.66c   0.00926
      29063.66c   0.176129
      29065.66c   0.078503
c
m11   2003.66c    0.8            $ Detector fill gas (He3 & Kr)
      36078.66c   0.0007         $ 2.471984E-04 @/b-cm
      36080.66c   0.0045
      36082.66c   0.0232
      36083.66c   0.023
      36084.66c   0.114
      36086.66c   0.0346
c
m12  82206.66c    2.45933E-01 $ Lead/air mix
     82207.66c    2.24434E-01 $ 8.07691E-03 @/b-cm
     82208.66c    5.29585E-01
      7014.60c    3.70514E-05
      8016.66c    9.93126E-06
     18000.59c    2.21197E-07
c
c source definition
c kcode 10000 0.7 1500 100
c ctme 840
nps 15E6
c
c Tally Definitions
c F44:n 425 435 445 455 465
c F64:n 625 635 645 655 665
c
c Mesh Tallies
fmesh14:n origin=-50.8 -50.8 29.74
            imesh=50.8      iints=100
            jmesh=50.8      jints=100
            kmesh=30.74     kints=  1
fmesh24:n origin=-50.8 -50.8 51.14
            imesh=50.8      iints=100
            jmesh=50.8      jints=100
            kmesh=52.14     kints=  1
fmesh34:n origin=-50.8 -50.8 72.54
            imesh=50.8      iints=100
            jmesh=50.8      jints=100
            kmesh=73.54     kints=  1
fmesh44:n origin=-50.8 -50.8 93.94
            imesh=50.8      iints=100
            jmesh=50.8      jints=100
            kmesh=94.94     kints=  1
fmesh54:n origin=-50.8 -50.8 115.34
            imesh=50.8      iints=100
            jmesh=50.8      jints=100
            kmesh=116.34    kints=  1
c
c weight card used for neutron dose calculation
c
sdef erg=d1 pos=0 -10.16 70.15097 axs=0 0 1 rad=d2 ext=d3
c
c erg based neutron energy spectrum of PuBe source
si1 h 0  .25
         .5
         .7
        1.0
        1.4
        1.75
        2.0
        2.5
        2.75
        3
```

```
        3.1
        3.25
        3.5
        4.0
        4.5
        4.75
        5.0
        5.5
        6.0
        6.5
        7.0
        7.75
        8.0
        8.5
        9.0
        9.5
        9.75
       10.0
       10.25
       10.5
       10.75
sp1 0    .06
         .045
         .055
         .045
         .05
         .04
         .055
         .09
         .155
         .22
         .24
         .205
         .19
         .185
         .195
         .19
         .17
         .13
         .02
         .115
         .07
         .11
         .10
         .05
         .02
         .035
         .05
         .04
         .03
         .0075
        0
si2 0 1.397
sp2 0 1
si3 0 6.4008
sp3 0 1
```

APPENDIX B

CANBERRA MODEL 0.5NH1/1K ^{3}HE NEUTRON DETECTOR DATA SHEET

CANBERRA

Helium-3 Neutron Detectors
10 mm diameter

Features

- Accurate localization of neutrons in neutron scattering

- 1 200 detectors 12NH25/1 on the TOF IN5 spectrometer of the RHF (ILL Grenoble-france)

- Measurement of soil dampness in petroleum drilling

- Active lengths: 1 cm, 12.5 cm, 25 cm (other lengths on request (for quantities above 10 pieces)

- Standard Helium-3 pressure: 8 bars, up to 20 bars on request (> 10 pieces)

- Active diameter: 9 mm

- Electrical output on wire, HV BNC or ATI

- Weight reduction of the detector+moderator system

- Excellent sensitivity-to-space ratio

Description

The 10 mm diameter neutron detectors allow accurate localization of neutrons.

These detectors are then widely used in neutron scattering experiments, around research nuclear reactors and neutron spallation sources. Angular position measurements and/or Time-of-Flight are performed simultaneously on large detection areas. For example, 1 200 12NH25/1 detectors have been installed on the historical TOF IN5 spectrometer of the Hifg Flux Reactor of the Laue-Langevin Institute at Grenoble.

For these neutron scattering applications, following characteristics have been optimized:
- very low background resulting from a severe selection of materials,
- very low jitter due to the choice of an appropriate gas mix,
- mechanical presentation adapted to the manufacturing of multi-element devices, with an electrical output on wire and a built-in mechanical binding.

The 10 mm diameter detectors are also used in the measurement of soil dampness in oil drilling; in that application, their excellent sensitivity-to-space ratio is of much interest.

The 0.5NH1/1K miniature and isotropic model is remarkable due to its very small size (active length 1 cm, diameter 1 cm) and its sensitivity (0.5 cps/nV); these characteristics make it a unique sensor for the equipment of light weight neutron monitors (as an example, in the dose rate meter-dosemeter DINEUTRON wighing only 3.5 kg).

Helium-3 Neutron Detectors
10 mm diameter

Specifications

■ MAIN MODELS

	Active length	Sensitivity	Capacity	Weight
	L in mm	c.s^{-1} per n.cm^{-2}.s^{-1}	pF	grams
0.5NH1/1K (F,I)	10	0.5	3	6 (20.13)
6NH12.5/1 (F)	125	6	4	29 (40)
12NH25/1 (F)	250	12	5	45 (56)

■ MECHANICAL

WALL
 Monel Ni-Cu (73-27)
 Width 0.5 mm
 Internal diameter 9 mm
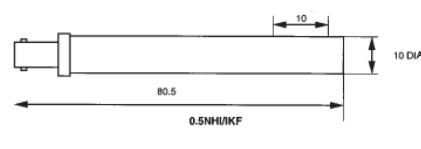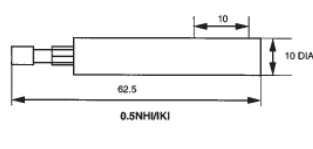
ELECTRICAL OUTPUT
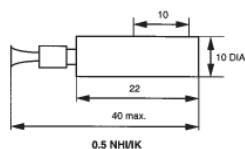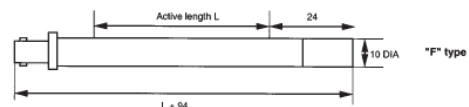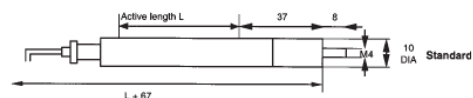 Standard output on nickel wire   : no suffix
 On request, HV BNC female connector   : suffix "F"
      M4015 ATI female connector   : suffix "I"

■ GAS FILLING

Helium 3 pressure	8	bars	600	cm Hg
Addition of krypton (0.5NH1/1K)	2	bars	150	cm Hg

■ TYPICAL OPERATING CHARACTERISTICS

ACHEM7F CHARGE AMPLIFIER
 C_{eq} 0.05 pF, Discrimination 125 mV, Integration 1 μs, Differentiation 4 μs

	6NH12.5/1 12 NH25/1	0.5NH1/1K (F,I) Isotropic	Unit
Mean high voltage (A~15)	1 150	1 600	V
Dispersion of gas amplification	±5	-	%
Length of the high voltage plateau	250	100	V
Slope of the high voltage plateau	0.6	5	% per 100 V
FWHM resolution	5	-	%
Jitter	0.3	0.3	μs
Pulse rise time	0.6	0.6	μs
Background with protection	6	30	c.h^{-1}.

VITA

   Lucas Tucker was born January 14, 1987, in Louisville, Kentucky. He earned a B.S. in Nuclear Engineering from Missouri University of Science and Technology in May 2009. He continued his study of nuclear engineering at Missouri University of Science and Technology, becoming a graduate student in June 2009. Lucas intends to pursue a Ph.D. in nuclear engineering as well. He is a Chancellor's Fellow and is currently working on his dissertation on non-destructive techniques for discriminating MOX and LEU fuel assemblies. His teaching experience includes Nuclear Radiation Measurements Lab and Introduction to Nuclear Engineering. Lucas is a student member of the American Nuclear Society and Alpha Nu Sigma. He spends his free time volunteering for the Boy Scouts of America. Lucas graduated with an M.S. degree in July 2011.